P D Smith and R J Jarvis (Editors)
University of Dundee

Ordinary and partial differential equations Volume V

Proceedings of the thirteenth Dundee Conference, 1996

LONGMAN

Addison Wesley Longman Limited
Edinburgh Gate, Harlow
Essex CM20 2JE, England
and Associated Companies throughout the world.

Published in the United States of America
by Addison Wesley Longman Inc.

First published 1997

AMS Subject Classifications (Main) 34-06, 35-06
(Subsidiary) 78-06, 92-06

ISSN 0269-3674

ISBN 0 582 30589 6

British Library Cataloguing in Publication Data

A catalogue record for this book is
available from the British Library

Printed and bound in Great Britain
by Biddles Ltd, Guildford and King's Lynn

P K MAINI

Propagating patterns in morphogenesis and wound healing

This paper considers two very different aspects of propagating patterns in biology and medicine. The first concerns the development of multicellularity in the life cycle of the microorganism *Dictyostelium discoideum*, which provides a paradigm model system for the study of pattern formation. Following starvation, periodic waves of the chemical cyclic AMP initiate the aggregation of *Dictyostelium* amoebae, via a cell streaming mechanism. A coupled cell-chemical, chemotaxis-reaction-diffusion model is presented and shown to exhibit aggregation as the consequence of the growth of a small-amplitude pattern in cell density forced by the large amplitude cAMP waves.

The second concerns scar formation in adult dermal wounds. A crucial factor in determining the degree of scarring is the ratio of types I and III collagen. A reaction-diffusion model which focuses on the control of collagen synthesis by key growth factors is considered. Numerical simulations of the spatially independent version of the model lead to values of the collagen ratio consistent with those observed experimentally. However, numerical simulations of the reaction-diffusion system do not exhibit this sensitivity to chemical application. Mathematically, this corresponds to the observation that behind healing wave front solutions, a particular healed state is always selected, independent of transients, even though there is a continuum of possible steady states.

1. Introduction.

One of the major issues in developmental biology is the formation of spatial and spatiotemporal pattern within the developing embryo. From the almost uniform mass of dividing cells in the very early stage of development, emerges the vast range of pattern and structure observed in animals. Many mathematical models have been

proposed to account for this phenomenon in a number of contexts. For example, in the developing vertebrate limb bud, the spatial pattern of skeletal elements is laid down in a specific spatiotemporal sequence beginning with the humerus, then radius and ulna, and then the digits (see Maini and Solursh, 1991, for a review of experimental results and theoretical models). In the dorsal area of the chick, feather germs are laid down, first along the dorsal midline, and then along adjacent parallel rows leading to a rhombic spatial pattern in germs (Cruywagen and Murray, 1992, Cruywagen *et al.*, 1992). Hair follicles also occur in a spatiotemporal fashion (Nagorcka, 1995a, b). In the alligator, stripes of coloration propagate downwards from the neck (Murray *et al.*, 1990) while tooth primordia in the alligator are formed in a complex spatiotemporal sequence (Kulesa *et al.*, 1996). Temporal patterns are well-known in the Belousov-Zhabotinskii chemical reaction (see the book by Murray, 1989 and references therein) and spatial patterns have been observed in the chloride-iodide-malonic acid reaction (Castets *et al.*, 1990; Ouyang and Swinney, 1991).

Spatiotemporal patterns are observed in other areas of nature (Maini, 1995, 1996). For example, propagating patterns occur as waves of invasion, either in population dynamics, where a population moves into a region (see, Murray, 1989 and references therein) or in wound healing, where cells move into a wound to close it.

To illustrate the diverse nature and role of propagating patterns in this area we focus on two examples. In Section 2 we consider pattern formation in *Dictyostelium discoideum* and in Section 3 we present a model for scar formation during wound healing.

2. A Model for Cell Aggregation in Slime Mold.

The life cycle of the cellular slime mould *Dictyostelium discoideum* serves as an excellent paradigm for morphogenesis and has, over the past 50 years, attracted the interest of developmental biologists and theoreticians alike. Under favourable conditions, the amoebae feed on bacteria in the soil and divide. Starvation triggers a developmental programme which leads to the formation of a multicellular organism

composed typically of $10^4 - 10^5$ cells. This organism passes through an intermediate motile (slug) phase during which cells differentiate into pre-spore and pre-stalk types, before developing a fruiting body, aiding the dispersal of spores from which, under favourable conditions, new amoebae develop. The comparative simplicity of morphogenesis in *Dictyostelium* has made it an attractive model system for the study of self-organisation, and many of the molecular and cellular mechanisms which are involved in cell aggregation, collective movement and differentiation have now been identified.

Three key steps are involved in aggregation. Firstly, cells signal to each other via the extracellular messenger cyclic 3'5'-adenosine monophosphate (cAMP), which propagates through the medium in the form of concentric and spiral concentration waves. Secondly, cells respond to cAMP moving chemotactically in periodic steps towards the aggregation centre (Alcantara and Monk, 1974; Tomchik and Devreotes, 1981). Thirdly, the onset of multicellularity is marked by the appearance of a branching pattern of cell streams in which direct cell-cell contacts are established.

The elucidation of the molecular mechanisms of the cAMP signalling dynamics since the 1980's (e.g. Devreotes 1989 and references therein) was accompanied by the development of mechanistic models of cAMP signalling. These models incorporate the detailed biochemical dynamics of the binding of extracellular cAMP to its surface receptors, and concentrate in detail on the temporal aspects of signalling (see, for example, Martiel and Goldbeter, 1987; Monk and Othmer, 1989; Tang and Othmer, 1994; Goldbeter, 1996).

The incorporation of diffusion of extracellular cAMP into these models yields a description of the signalling dynamics in a stationary cell layer, which is a valid approximation for the situation at the beginning of cell aggregation (Tyson *et al.*, 1989; Monk and Othmer, 1990; Tang and Othmer, 1995). Within the framework of the resultant system of coupled reaction-diffusion equations, the experimentally observed cAMP waves can be viewed as a particular case of waves in so-called excitable media

(Tyson and Murray, 1989). However, the signalling models neglect cell movement and thus can not describe the actual aggregation process and in particular cell streaming.

It is intuitively clear that the dynamics of the cell distribution and of cAMP signalling are closely coupled: cell movement is induced by the cAMP waves, while cells themselves act as sources and sinks for cAMP. A number of early models were proposed to describe the aggregation process in slime mould (Keller and Segel, 1970; Cohen and Robertson, 1971a,b; Parnas and Segel, 1977, 1978; MacKay, 1978). These were largely based on phenomenological observations of the aggregation dynamics. However, the increased understanding of cAMP signalling at the molecular level, provides the opportunity of extending these detailed models of cAMP dynamics to include cell-cAMP interactions. Recently, this problem has been tackled in two different ways. The first approach consists of modelling discrete cells equipped with cAMP-dependent movement rules coupled to a finite-difference approximation for the continuous cAMP dynamics (Dallon and Othmer, 1996; Van Oss *et al.*, 1996; Kessler and Levine 1993). A second approach, is to approximate the cell distribution by a continuous density, resulting in a system of coupled partial differential equations for the cell density and the cAMP dynamics (Vasiev *et al.*, 1994; Höfer *et al.*, 1995a,b).

In this paper, we focus on the continuum model of Höfer *et al.*, 1995a. The model takes the following form

$$\frac{\partial n}{\partial t} = \nabla \cdot (\mu \nabla n - \chi(v) n \nabla u) \tag{1}$$

$$\frac{\partial u}{\partial t} = \lambda[\phi(n) f_1(u,v) - (\phi(n) + \delta) f_2(u)] + \nabla^2 u \tag{2}$$

$$\frac{\partial v}{\partial t} = -g_1(u)v + g_2(u)(1-v), \tag{3}$$

where n, u and v denote cell density, extracellular cAMP concentration and fraction of active cAMP receptors, respectively. We motivate each equation in turn. Equation (1) is the conservation equation for cell density. The first term models random cell movement with a constant cell diffusion coefficient μ. The second term models

chemotaxis, the name given to movement up gradients in chemical concentration. A critical aspect of the modelling is the form of $\chi(v)$, the chemotactic cell sensitivity. We assume that this term depends on the fraction of active cAMP receptors per cell and takes the form $\chi(v) = \chi_0 v^m/(A^m + v^m)$, $m > 1$, where χ_0 and A are positive constants. This accounts for the adaptation of the chemotactic machinery of the cells (Devreotes and Zigmond, 1988) in the following way: an appreciable chemotactic response requires a minimal fraction of active receptors, yet, for a large fraction of active receptors, the response saturates. Note that many models of chemotaxis assume χ to be a constant. Under that assumption, cells would respond to a pulse of chemoattractant by moving towards the wave in the wavefront, then moving with the wave in the waveback, resulting in a net movement away from the source of attractant, rather than towards it. This is the so-called "chemotactic wave paradox" (Soll *et al.*, 1993). The form of $\chi(v)$ chosen above resolves this paradox (Höfer *et al.*, 1994).

Equation (2) models extracellular cAMP concentration. For computational simplicity, slightly simplified algebraic versions of the kinetic terms derived by Martiel and Goldbeter, 1987, are used, which, nevertheless, retain the important biochemical characteristics of the latter. The rate of cAMP synthesis per cell is modelled by $f_1(u, v) = (bv + v^2)(a + u^2)/(1 + u^2)$. This models autocatalytic cAMP production with saturation, mediated by cAMP binding to active receptors. The rate of cAMP degradation per cell is taken to be $f_2(u) = du$. The cell density dependence is reflected in the factor $\phi(n) = n/(1 - \rho n/(K + n))$, while δ accounts for cAMP degradation in the absence of cells (see Höfer *et al.*, 1995a, for full details). The parameters a, b, d, ρ, K, δ and λ are all positive constants.

Similarly, in (3), the rate functions of receptor desensitization and resensitization are simplified expressions of the corresponding terms in the Martiel-Goldbeter model. In the first term on the right hand side, $g_1(u) = k_1 u$, so that receptor desensitization in the presence of cAMP satisfies the law of mass action. The second term on the

right hand side models resensitization of the desensitized $(1-v)$ fraction of receptors, at the constant rate $g_2(u) = k_2$. The parameters k_1 and k_2 are positive constants.

Good estimates of most of the parameters are available from the experimental literature (see Höfer *et al.*, 1995b) and, substituting these values into the model, we find that the model captures the key features of the aggregation process. A typical aggregation sequence is shown in Figure 1.

Periodic wave solutions of the model can be analysed by converting (1)-(3) to travelling wave coordinates, yielding the system of ordinary differential equations:

$$c(N - n_0) + \mu\frac{dN}{dz} - \chi(V)N\frac{dU}{dz} = 0 \quad (4)$$

$$\frac{d^2U}{dz^2} + c\frac{dU}{dz} + \lambda f(N,U,V) = 0 \quad (5)$$

$$c\frac{dV}{dz} + g(U,V) = 0, \quad (6)$$

where $f(N,U,V) = \phi(N)f_1(U,V) - (\phi(N)+\delta)f_2(N)$, $g(U,V) = g_1(U)V + g_2(U)(1-V)$, $z = x - ct$, and $n(x,y,t) = N(z) = N(z+\Lambda)$, etc., where c and Λ denote wave speed and wavelength, respectively, and n_0 is the unperturbed homogeneous cell density.

From parameter estimates, $\mu \ll \chi_0$, so (4) can be approximated by $N(z) = \frac{n_0 c}{c - w(z)}$, where $w(z) = \chi(V(z))\frac{dU}{dz}$ is the average chemotactic velocity. As it is known from experiment that $\frac{w}{c} \leq 0.1$, this predicts that the homogeneous cell density is perturbed in the wavefront by about 10%. This is consistent with the experimental observation that during the initial stages of aggregation the amoebae are almost homogeneously distributed, and movement in response to the cAMP waves does not result in noticeable changes in cell density (Alcantra and Monk, 1974).

Our numerical simulations indicate that large-amplitude wave propagation in one space dimension is a stable phenomenon. To investigate the stability of wave propagation in two space dimensions for the full model (1)-(3), we add small perturbations to the solutions of (4)-(6) of the form $n(x,y,t) = N(z) + \hat{n}(z,y)$. This assumes a special form of perturbation which has only implicit time dependence via z. We mo-

tivate this as follows. As wave propagation in the subsystem (2)-(3), with $\phi(n) \equiv 1$ and $\delta = 0$, is stable, any possible instability must be linked to the dynamics of cell movement. These are forced by the cAMP waves, which may cause non-uniformities in cell density to grow. These homogeneities will not propagate with the waves, however, as $w \ll c$. Therefore we expect a perturbation to evolve in the travelling wave frame. This is confirmed by a power spectrum analysis of numerical simulations of the equations (see Höfer *et al.*, 1995b, for full details). Looking for separable solutions of the form $\mathbf{a}(z)exp(iqy)$ to the resultant equations for the perturbations leads to a second order differential equation system for the components of $\mathbf{a}$ with periodic coefficients. The Floquet multipliers of the system have to be calculated numerically and the largest multiplier can be used to obtain the dispersion relation for patterning in the y-direction. It is found that the initial uniform state is unstable from the outset, suggesting that the coupled dynamics of cAMP wave propagation and cell movement exhibit a patterning instability perpendicular to the direction of wave propagation. The dispersion relation predicts the wavelength of the fastest growing unstable mode, and agrees closely with the results of numerical simulations and experimental observations.

An analytically-tractable caricature of the above model has been proposed by Höfer *et al.*, 1995b, from which it is possible to derive explicit conditions on the parameters for the uniform steady state to go unstable.

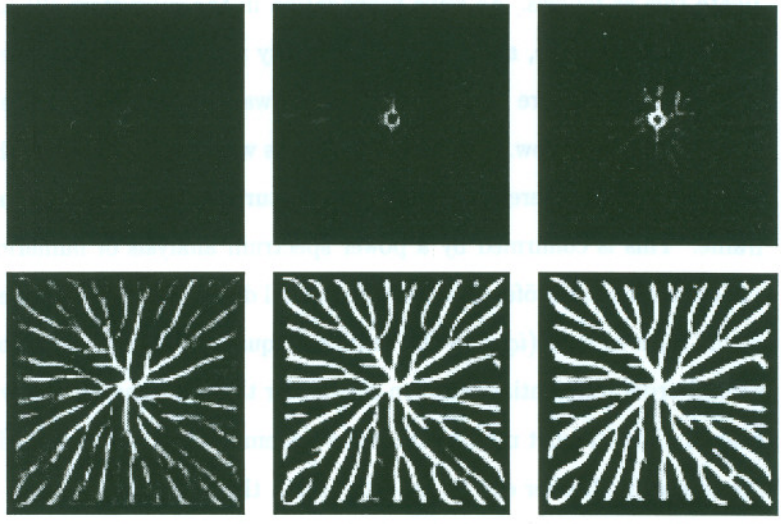

(a)

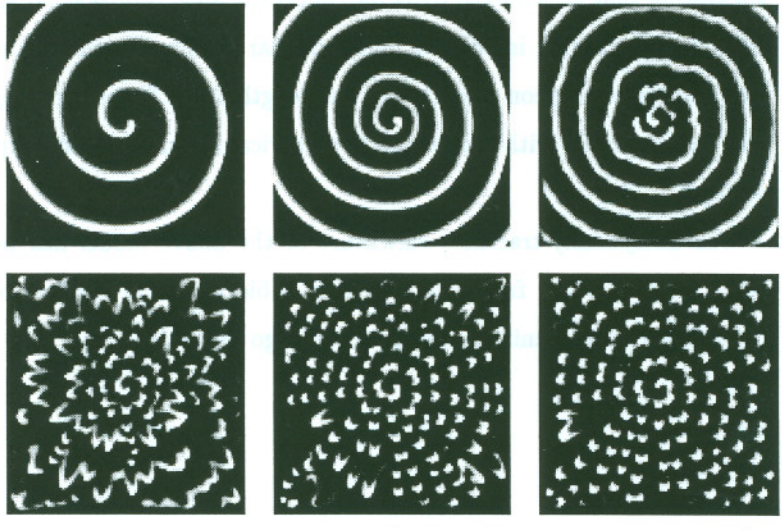

(b)

Figure 1 Numerical solution to (1)-(3). (a) Cell density, (b) cAMP concentration. Snapshots are taken at t=12 min, 22 min, 32 min, 52 min, 72 min and 112 min (left to right, top to bottom). For parameter values, see Höfer, 1996.

Therefore, the comparatively simple model (1)-(3) can capture, both qualitatively and quantitatively, the key aspects of spatiotemporal patterning in *Dictyostelium* aggregation. The instability leading to cell streaming is similar to that found in other biological pattern formation models in that spatial modes associated with a real eigenvalue (or, in this case, Floquet exponent) go unstable. However, the route to pattern formation is different to that in the standard models. The pattern is forced by the cAMP waves of the reaction-diffusion sub-system (2)-(3) and acts as a dynamical pre-pattern resulting in cell patterning in streams perpendicular to the wavefronts. This provides a case study for the coupling of two biologically implicated patterning mechanisms, reaction-diffusion and chemotaxis.

A more detailed numerical study of the model reveals a number of other important properties. For example, as cell streams grow, they alter the propagation conditions for the cAMP waves. This is initially equivalent to increasing λ, leading to an increase in excitability of the medium. This, in turn, leads to an increase in the rotation frequency of the spiral core. As a result (Tyson and Keener, 1988) the wavespeed and wavelength of the spiral patterns decrease. This is typical of *Dictyostelium* spiral patterns *in situ* (Gross *et al.*, 1976) and has, previously, been explained by assuming that biochemical changes must be occurring in the cell-cAMP system. Although this may be the case, our results show that such changes are not necessary to explain the phenomena observed. Our numerical simulations also show that low initial cell densities lead to the formation of a central hole. The formation of a central hole is observed experimentally, if the system is treated with caffeine (Steinbock and Müller, 1995). Caffeine treatment lowers the excitability of the system which corresponds, in the model (1)-(3), to lowering λ. From equation (2) this is equivalent, in some sense, to lowering the cell density n.

We conclude that this minimal model, based on biochemical and mechanical mechanisms established at the cellular level, has captured in some detail the cell movement and chemical signalling dynamics observed experimentally. Moreover, it provides a

further link between properties at the individual cell level and the collective patterning modes of the population of cells at the onset of multicellular organisation.

3. Scar Tissue Formation.

Recent advances in molecular and cellular biology have led to the rapid development of experimental research into the biochemical mechanisms underlying the process of wound healing. Increasingly, mathematical modelling is playing a crucial role by providing a theoretical framework in which these experimental results can be understood. The study of propagating waves is essential in this context as, in many cases, a crucial aspect of healing involves cells moving into a wound to close it (Dale *et al.*, 1994, 1996a; Olsen *et al.*, 1995, 1996).

In this section we consider a model for scar formation (for full details, see Dale *et al.*, 1996b,c). Adult dermal wounds, in contrast to early foetal wounds, heal with the formation of scar tissue. Scar tissue is less functional than the surrounding undamaged tissue and is also weaker, so that the tissue can easily suffer more damage.

Dermal tissue contains two main types of collagen, types I and III. Two key differences between normal and scar tissue are the orientation of collagen fibres and their thickness. In unwounded dermis, the collagen fibres are arranged in a basketweave pattern, while in scar tissue, the fibres are oriented perpendicular to the basement membrane. The collagen fibres in scar tissue are longer and thinner than in normal tissue, due to higher levels of type III collagen (Mast *et al.*, 1992). As type III collagen decorates the surface of the type I collagen fibres, a higher ratio of type III to type I results in thinner fibres (Whitby and Ferguson, 1991). Therefore, one way to investigate the formation and control of scar tissue is to investigate how the ratio of collagen types I to III is determined during the healing process.

In response to injury, fibroblasts migrate into the wound domain and synthesize chains of amino acids called procollagens (McDonald, 1988). This process is activated by growth factors such as Transforming Growth Factor β (TGFβ) (Appling *et al.*, 1989). Enzymes activate the procollagens leading to the formation of collagen. At the

same time, fibroblasts synthesize zymogens, which when activated form collagenases. The model consists of sixteen variables – fibroblasts, four variables to account for the latent and active forms of TGFβ1 and 3, six variables to account for collagen types I and III and the associated procollagens and collagenases, two zymogens, and three activating enzymes.

The fibroblast population, f, is modelled by the equation

$$\frac{\partial f}{\partial t} = \overbrace{D_1\nabla^2 f}^{\text{Migration}} + \overbrace{(A_1 + A_2\beta_1 + A_3\beta_3)f\left(1 - \frac{f}{k}\right)}^{\text{Mitotic Generation}} - \overbrace{A_4 f}^{\text{Natural Loss}} . \tag{7}$$

The first term models movement of fibroblasts from unwounded tissue by Fickian diffusion, with constant coefficient, D_1. There are two possible sources of fibroblasts – the surrounding unwounded dermal tissue, and the underlying subcutaneous tissue. The exact source is an area of much biological debate. We assume that the fibroblast population obeys a logistic growth law in which the linear growth rate is enhanced by the presence of TGFβ1 and 3, concentrations β_1 and β_3, respectively (Krummel *et al.*, 1988).

TGFβ1 is assumed to satisfy the equation

$$\frac{\partial \beta_1}{\partial t} = \overbrace{D_2\nabla^2\beta_1}^{\text{Chemical Diffusion}} + \overbrace{A_5 e_1 l_1}^{\text{Activation}} - \overbrace{A_6\beta_1}^{\text{Natural Decay}} , \tag{8}$$

where we use the law of mass action to model activation of latent TGFβ1 (concentration l_1), by the enzyme e_1 (Sinclair and Ryan, 1994). Experiments have shown that active TGFβ undergoes rapid decay, which we model as a first order process (Roberts and Sporn, 1990).

Similarly, TGFβ3 satisfies the equation

$$\frac{\partial \beta_3}{\partial t} = D_3\nabla^2\beta_3 + A_7 e_1 l_3 - A_8\beta_3, \tag{9}$$

where l_3 is the concentration of latent TGFβ3.

The latent forms l_1 and l_3 are, in turn, taken to satisfy the equations

$$\frac{\partial l_1}{\partial t} = \overbrace{D_4\nabla^2 l_1}^{\text{Diffusion}} + \overbrace{\frac{A_9 f l_1}{1 + A_{10}l_3 + A_{11}l_1}}^{\text{Production by Fibroblasts}} - \overbrace{A_{12}l_1}^{\text{Natural Decay}} - \overbrace{A_{13}e_1 l_1}^{\text{Activation}} \tag{10}$$

and

$$\frac{\partial l_3}{\partial t} = D_5 \nabla^2 l_3 + \frac{A_{14} f l_3}{1 + A_{15} l_3} - A_{16} l_3 - A_{17} e_1 l_3, \tag{11}$$

respectively. The latent forms of TGFβ are secreted by the fibroblasts, stimulated by the corresponding growth factors (Wakefield *et al.*, 1988), but their production does not increase unboundedly, hence the saturating functional form. Latent TGFβ also undergoes an autocrine mechanism, whereby it induces self-secretion (Roberts and Sporn, 1990). Natural decay is modelled as a first order process (Wakefield, *et al.*, 1990). Activation by specific enzymes decreases the concentration of the latent growth factors.

The enzymes, e_1, e_2 and e_3 satisfy the equations

$$\frac{de_1}{dt} = -e_1(A_{13} l_1 + A_{17} l_3) \tag{12}$$

$$\frac{de_2}{dt} = -e_2(A_{18} p_1 + A_{19} p_3) \tag{13}$$

$$\frac{de_3}{dt} = -e_3(A_{20} z_1 + A_{21} z_3). \tag{14}$$

The procollagens, concentrations p_1 and p_3, are synthesized by the fibroblasts (Miller and Gay, 1992) but do not diffuse. We assume that the production rate is increased by the growth factors, in line with experimental observations (Appling *et al.*, 1989). Modelling natural decay as a first order process, the equations are

$$\frac{dp_1}{dt} = (A_{22} + A_{23}\beta_1 + A_{24}\beta_3) f - A_{25} p_1 - A_{18} e_2 p_1 \tag{15}$$

$$\frac{dp_3}{dt} = (A_{26} + A_{27}\beta_1 + A_{28}\beta_3) f - A_{29} p_3 - A_{19} e_2 p_3. \tag{16}$$

The third terms on the right hand side of both the above equations model conversion of procollagen by enzyme e_2 to collagen. The collagens themselves are degraded by the collagenases. As there is no experimental evidence for significant movement of intact collagen fibres, we therefore have the following equations for collagen type I, c_1, and type III, c_3

$$\frac{dc_1}{dt} = A_{30} p_1 e_2 - A_{31} s_1 c_1 \tag{17}$$

$$\frac{dc_3}{dt} = A_{32}p_3e_2 - A_{33}s_3c_3. \tag{18}$$

Collagenases I and III, concentrations s_1 and s_3, respectively, are the active form of zymogens I and III, which arise via enzymatic activation. Therefore, they satisfy the equations

$$\frac{ds_1}{dt} = A_{34}z_1e_3 - A_{35}s_1 \tag{19}$$

$$\frac{ds_3}{dt} = A_{36}z_3e_3 - A_{37}s_3. \tag{20}$$

Finally, the zymogens, concentrations z_1 and z_3, are synthesized and secreted by the fibroblasts but the secretion is inhibited by the presence of active TGFβ (Jeffrey, 1992). Taking the natural decay of zymogens to be first order, and including the loss of zymogen due to activation to collagenase by enzyme e_3, we have

$$\frac{dz_1}{dt} = \frac{A_{38}}{1 + A_{39}\beta_1 + A_{40}\beta_3} f c_1 - A_{41}z_1 - A_{20}e_3z_1 \tag{21}$$

$$\frac{dz_3}{dt} = \frac{A_{42}}{1 + A_{43}\beta_1 + A_{44}\beta_3} f c_3 - A_{45}z_3 - A_{21}e_3z_3. \tag{22}$$

Equations (7)-(22) constitute the model, and k, $D_1 ... D_5, A_1 ... A_{45}$ are constant parameters. The estimation of dimensional parameter values is essential for biologically realistic model predictions. The governing equations contain a large number of parameters whereas there is a limited source of experimental data. However, we know the time scale of the healing process and can hence obtain order of magnitude estimates for some of the remaining parameters (see Dale, *et al.*, 1996b). Note that, at steady state $s_1 = s_3 = 0$. Therefore, from (17) and (18) there is a continuum of steady states for c_1 and c_3.

The model is applied to "slash" wounds, in which the length of the wound is much greater than its depth or width. Therefore, to a good approximation, the wound can be represented by a one-dimensional domain, with zero flux boundary conditions for the diffusing variables and Dirichlet conditions for the other variables, fixed at steady state. The wounded domain can be normalised to be the unit interval.

However, to fully investigate the properties of the propagating solutions to (7)-(22) it is necessary to solve the system on a large spatial domain. Numerical solutions of the model equations for parameters appropriate to the foetal case show waves of cells and growth factors moving into the wound with constant speed and shape, with the steady states corresponding to the unwounded nondimensional level (Figure 2). The solution profiles for collagen I and III also show fronts moving into the wound domain, evolving to new steady state levels for both collagen I and III, with a ratio of 3:1, in agreement with the unwounded dermal tissue. The collagenase equations show wave pulses moving into the wounded domain and both collagenase I and III decay to the zero dermal level. Solutions for parameters appropriate for the adult case again exhibit travelling waves, but in this case the ratio of collagen I to III coresponds to thinner collagen fibres and thus scar tissue formation.

The model, therefore, captures a crucial aspect of dermal wound healing, namely that adult wounds heal by scarring, while early foetal wounds heal with substantially reduced scar tissue formation. A further test of the model is to consider the effect of altering the amount of TGFβ1 by changing the initial conditions. For the case of the model with all diffusion coefficients set to zero, the final levels of collagen I and III predicted by the model suggest that addition of TGFβ1 results in increased scarring. This is what is observed experimentally (Shah *et al.*, 1992). The model predicts that topical application of TGFβ3 increases the amount of collagen I compared to type III, thus causing thicker fibres and a reduction in scar tissue. Furthermore, numerical solutions show that early addition of growth factor is essential for effective control of scar tissue formation.

The model framework above can be used to investigate the source of fibroblasts. Numerically, we find that diffusion of fibroblasts into the wound from surrounding undamaged tissue appears to select and stabilise a unique steady state for c_1 and c_3, regardless of the initial conditions. This contradicts experimental observations. However, if the underlying tissue is the source of fibroblasts, so that $D_1 = 0$ in (7)

but initially the wound is seeded with fibroblasts from below, then the final steady state values do depend on the initial conditions and are consistent with experimental observations.

We can understand this behaviour by considering the following analytically-tractable caricature model

$$\frac{\partial u}{\partial t} = D\frac{\partial^2 u}{\partial x^2} + u(1-u) \tag{23}$$

$$\frac{\partial v}{\partial t} = \alpha u(1-u) - (1-u)v, \tag{24}$$

where D and α are positive constants. Equation (23) is the Fisher equation (Fisher, 1937) and decouples from (24). This mimics the fact that, in the full model, (7)-(12) decouple from (13)-(22). Moreover, in addition to the trivial steady state $(0,0)$, there is a continuum of steady states $(1, v^*)$ where v^* can take any value. For the case $D = 0$, (23) and (24) can be solved easily for the initial conditions $u = u_0, v = 0$ and, as $t \to \infty, u \to 1$ and $v \to v^* \equiv \alpha(1-u_0^2)/2$.

For the case where D is non-zero, the corresponding travelling wave problem is

$$D\frac{d^2U}{dz^2} + c\frac{dU}{dz} + U(1-U) = 0 \tag{25}$$

$$c\frac{dV}{dz} + \alpha U(1-U) - (1-U)V = 0, \tag{26}$$

where $z = x - ct, u(x,t) = U(z)$, etc and c denotes the wavespeed. Far behind the wave, U is at the unwounded state $U(-\infty) = 1$, while far ahead of the wave $U(+\infty) = 0$. These conditions determine U uniquely from equation (25). Therefore, with the condition $V(+\infty) = 0$, equation (26) determines, for a fixed value of c, a unique value of V far behind the wave, that is, a unique healed steady state. An analytic approximation to this value can be found and is given by

$$v^* = \frac{\alpha}{2} + \frac{\alpha D}{12c^2} \tag{27}$$

(see Dale *et al.*, 1996c, for full details).

However, if the underlying tissue is the source of fibroblasts, so that $D_1 = 0$ in (7) but initially the wound is seeded with fibroblasts from below, then the final steady state values do depend on the initial conditions and are consistent with experimental observations.

We can understand this behaviour by considering the following analytically-tractable caricature model

$$\frac{\partial u}{\partial t} = D\frac{\partial^2 u}{\partial x^2} + u(1-u) \tag{23}$$

$$\frac{\partial v}{\partial t} = \alpha u(1-u) - (1-u)v, \tag{24}$$

where D and α are positive constants. Equation (23) is the Fisher equation (Fisher, 1937) and decouples from (24). This mimics the fact that, in the full model, (7)-(12) decouple from (13)-(22). Moreover, in addition to the trivial steady state $(0,0)$, there is a continuum of steady states $(1, v^*)$ where v^* can take any value. For the case $D = 0$, (23) and (24) can be solved easily for the initial conditions $u = u_0, v = 0$ and, as $t \to \infty, u \to 1$ and $v \to v^* \equiv \alpha(1-u_0^2)/2$.

For the case where D is non-zero, the corresponding travelling wave problem is

$$D\frac{d^2U}{dz^2} + c\frac{dU}{dz} + U(1-U) = 0 \tag{25}$$

$$c\frac{dV}{dz} + \alpha U(1-U) - (1-U)V = 0, \tag{26}$$

where $z = x - ct, u(x,t) = U(z)$, etc and c denotes the wavespeed. Far behind the wave, U is at the unwounded state $U(-\infty) = 1$, while far ahead of the wave $U(+\infty) = 0$. These conditions determine U uniquely from equation (25). Therefore, with the condition $V(+\infty) = 0$, equation (26) determines, for a fixed value of c, a unique value of V far behind the wave, that is, a unique healed steady state. An analytic approximation to this value can be found and is given by

$$v^* = \frac{\alpha}{2} + \frac{\alpha D}{12c^2} \tag{27}$$

(see Dale *et al.*, 1996c, for full details).

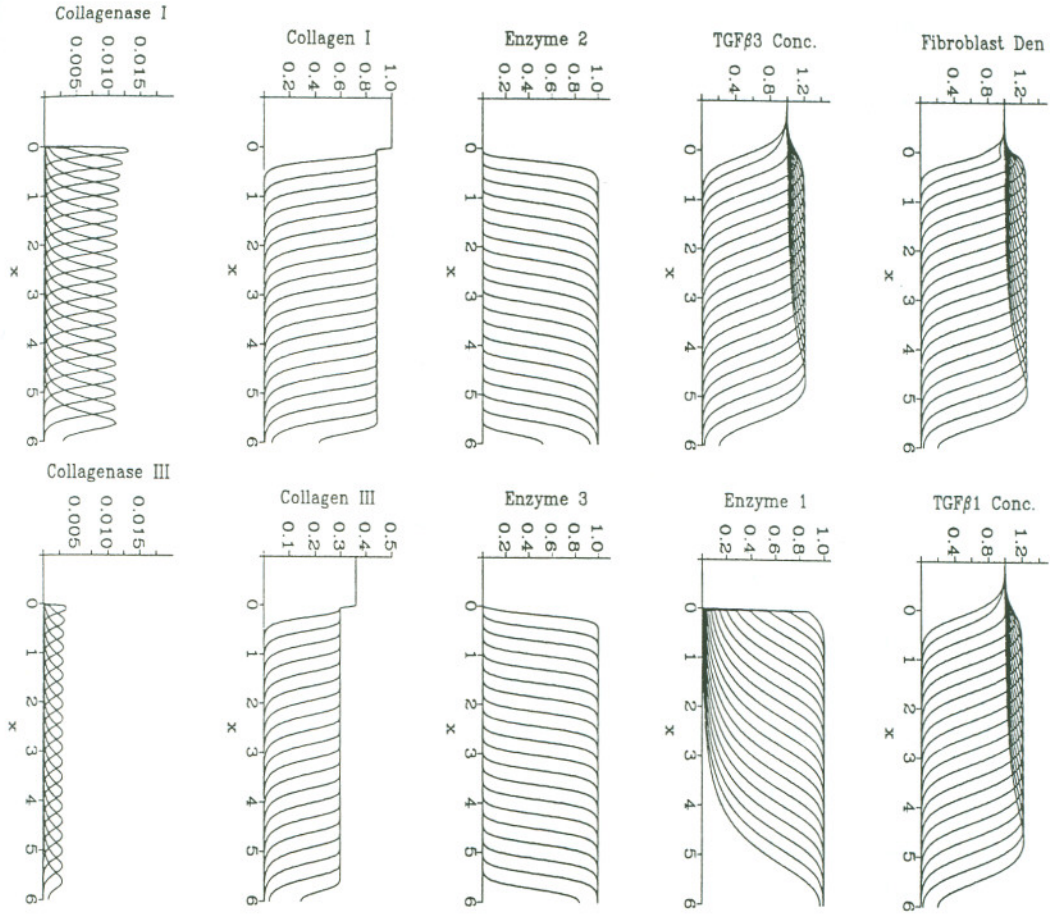

Figure 2 Numerical solution of equations (7)-(22) in one dimensional space, with zero flux boundary conditions. We impose step function initial conditions, with the model variables at their normal dermal level outside the wound domain. The field variables move into the wound as travelling waves and the ratio of collagen types I to III is 3:1. For parameter values, see Dale *et al.*, 1996a.

This simple caricature model, therefore, enables us to understand the behaviour of the full model and helps to shed light on the role of fibroblast migration in collagen formation.

4. Discussion.

In this paper we have illustrated the key role that propagating patterns play in biology and medicine by reviewing, in detail, two recently proposed mathematical models for two very different problems. The first application concerned aggregation in *Dictyostelium discoideum* and involved cell-chemotaxis driven by reaction-diffusion waves. The second concerned scar tissue formation as a consequence of the dynamics of collagen secretion driven by waves of cells propagating into the wound.

References

Alcantara, F and Monk, M (1974) Signal propagation during aggregation in the slime mold *Dictyostelium discoideum*, J. Gen. Microbiol., 85, 321-334

Appling, W D, O'Brien, W R, Johnston, D A and Duvie, M (1989) Synergistic enhancement of type I and III collagen production in cultured fibroblasts by transforming growth factor - β and ascorbate, FEBS Letters, 250, 541-544

Castets, V, Dulos, E, Boissonade, J and de Kepper, P (1990) Experimental evidence of sustained standing Turing-type nonequilibrium chemical pattern, Phys. Rev. Letters, 64, 2953-2956

Cohen, M H and Robertson, A (1971a) Wave propagation in the early stages of aggregation of cellular slime molds, J. theor. Biol., 31, 101-118

Cohen, M H and Robertson, A (1971b) Chemotaxis and the early stages of aggregation of cellular slime molds, J. theor. Biol., 31, 119-130

Cruywagen, G C and Murray, J D (1992) On a tissue interaction model for skin pattern formation, J. Nonlinear Sci., 2, 217-240

Cruywagen, G C, Maini, P K and Murray, J D (1992) Sequential pattern formation in a model for skin morphogenesis, IMA J. Math. Appl. Med. & Biol., 9, 227-248

Dale, P D, Maini, P K and Sherratt, J A (1994) Mathematical modelling of corneal epithelial wound healing, Math. Biosci., 124, 127-147

Dale, P D, Olsen, L, Maini, P K and Sherratt, J A (1996a) Travelling waves in wound healing, FORMA, 10, 205-222

Dale, P D, Maini, P K and Sherratt, J A (1996b) A mathematical model for collagen fibre formation during foetal and adult dermal wound healing, Proc. Roy. Soc. Lond. B 263, 653-660

Dale, P D, Maini, P K and Sherratt, J A (1996c) The role of fibroblast migration in collagen fibre formation during faetal and adult dermal wound healing (submitted)

Dallon, J C and Othmer, H G (1996), A discrete cell model with adaptive signalling for aggregation of *Dictyostelium discoideum*, Phil. Trans. Roy. Soc. Lond. B (to appear)

Devreotes, P N (1989) *Dictyostelium discoideum*: a model system for cell-cell interactions in development, Science, 245, 1054-1059

Devreotes, P N and Zigmond, S H (1988) Chemotaxis in eukaryotic cells: a focus on leukocytes and *Dictyostelium*, A. Rev. Cell Biol., 4, 649-686

Fisher, R A (1937) The wave of advance of advantageous genes, Ann. Eugenics, 7, 353-369

Goldbeter, A. (1996) *Biochemical Oscillations and Cellular Rhythms*, Cambridge University Press

Gross, J D, Peacey, M J and Trevan, D J (1976) Signal emission and signal propagation during early aggregation in *Dictyostelium discoideum*, J. Cell Sci., 22, 645-656

Höfer, T (1996) *Modelling Dictyostelium Aggregation*, D Phil thesis, Oxford

Höfer, T, Maini, P K, Sherratt, J A, Chaplain, M A J, Chauvet, P, Metevier, D, Montes, P C and Murray, J D (1994) A resolution of the chemotactic wave paradox, Appl. Math. Lett., 7, 1-5

Höfer, T, Sherratt, J A and Maini, P K (1995a) *Dictyostelium discoideum*: cellular self-organization in an excitable biological medium, Proc. Roy. Soc. Lond. B 259, 249-257

Höfer, T, Sherratt, J A and Maini, P K (1995b) Cellular pattern formation during *Dictyostelium* aggregation, Physica D, 85, 425-444

Jeffrey, J J (1992) Collagen degradation, In *Wound Healing: Biochemical and Clinical Aspects*, Cohen, I K, Diegelmann, R F and Lindblad, W J (eds.), W. B. Saunders Co., Philadelphia, pp. 177-194

Keller, E F and Segel, L E (1970) Initiation of slime mold aggregation viewed as an instability, J. theor. Biol., 26, 399-415

Kessler, D A and Levine, H (1993) Pattern formation in *Dictyostelium* via the dynamics of cooperative biological entities, Phys. Rev. E 48, 4801-4804

Krummel, T M, Michna, B A, Thomas, B L, Sporn, M B, Nelson, J M, Salzberg, A M, Cohen, I K and Diegelmann, R F (1988) Transforming growth factor beta induces fibrosis in a fetal wound model, J. Pediatric Surgery, 23, 647-652

Kulesa, P M, Cruywagen, G C, Lubkin, S R, Maini, P K, Sneyd, J S, Ferguson, M W J and Murray, J D (1996) On a model mechanism for the spatial patterning of teeth primordia in the Alligator, J. theor. Biol. (to appear)

MacKay, S A (1978) Computer simulation of aggregation in *Dictyostelium discoideum*, J. Cell Sci., 33, 1-16

Maini, P.K. (ed) (1995) *Travelling Waves in Biology, Chemistry, Ecology and Medicine*, Part 1, FORMA, 10, 145-280

Maini, P.K. (ed) (1996) *Travelling Waves in Biology, Chemistry, Ecology and Medicine*, Part 2, FORMA, 11, 1-80

Maini, P K and Solursh, M (1991) Cellular mechanisms of pattern formation in the developing limb, Int. Rev. Cytology, 129, 91-133

Martiel, J-L and Goldbeter, A (1987) A model based on receptor desensitization for cyclic AMP signaling in *Dictyostelium* cells, Biophys. J., 52, 807-828

Mast, B A, Nelson, J M and Krummel, T M (1992) Tissue repair in the mammalian fetus. In *Wound Healing: Biochemical and Clinical Aspects*, Cohen, I K, Diegelmann, R F and Lindblad, W J (eds.), W. B. Saunders Co., Philadelphia, pp. 326-343

McDonald, J A (1988) Fibronectin: a primitive matrix, In *The Molecular and Cellular Biology of Wound Repair*, Clark, R A F and Henson, P M (eds.), Plenum Press, New York, pp. 405-436

Miller, E J and Gay, S (1992) Collagen structure and function. In *Wound Healing: Biochemical and Clinical Aspects*, Cohen, I K, Diegelmann, R F and Lindblad, W J (eds.), W. B. Saunders Co., Philadelphia, pp. 130-151

Monk, P B and Othmer, H G (1989) Cyclic AMP oscillations in suspensions of *Dictyostelium discoideum*, Phil. Trans. Roy. Soc. Lond. B 323, 185-224

Monk, P B and Othmer, H G (1990) Wave propagation in aggregation fields of the cellular slime mould *Dictyostelium discoideum*, Proc. R. Soc. Lond. B 240, 555-589

Murray, J D, Deeming, D C and Ferguson, M W J (1990) Size-dependent pigmentation-pattern formation in embryos of *Alligator mississippiensis*: time of initiation of pattern generation mechanism, Proc. R. Soc. Lond. B 239, 279-293

Murray, J D (1989) *Mathematical Biology*, Springer-Verlag

Nagorcka, B N (1995a) The reaction-diffusion (RD) theory of wool (hair) follicle initiation and development I. Primary follicles, Aust. J. Agric. Res., 46, 333-355

Nagorcka, B N (1995b) The reaction-diffusion (RD) theory of wool (hair) follicle initiation and development II. Original secondary follicles, Aust. J. Agric. Res., 46, 357-378

Olsen, L, Sherratt, J A and Maini, P K (1995) A mechanochemical model for adult dermal wound contraction and the permanence of the contracted tissue displacement profile, J. theor. Biol., 177, 113-128

Olsen, L, Sherratt, J A, and Maini, P K (1996) A mathematical model for fibro-proliferative wound healing disorders, Bull. Math. Biol., 58, 787-808

Ouyang, Q and Swinney, H L (1991) Transition from a uniform state to heaxagonal and striped Turing patterns, Nature, 352, 610-612

Parnas, H and Segel L A (1977) Computer evidence concerning the chemotactic signal in *Dictyostelium discoideum*, J. Cell Sci., 25, 191-204

Parnas, H and Segel L A (1978) A computer simulation of pulsatile aggregation in *Dictyostelium discoideum*, J. theor Biol., 71, 185-207

Roberts, A B and Sporn, M B (1990) The transforming growth factor - βs, In *Peptide Growth Factors and their Receptors*, Sporn, M B and Roberts, A B (eds.), Springer Verlag, Berlin, pp. 419-472

Sinclair, R D and Ryan, T J (1994) Proteolytic enzymes in wound healing: the role of enzymatic debridement, Australas. J. Dermatol., 35, 35-41

Shah, M, Foreman, D M and Ferguson, M W J (1992) Control of scarring in adult wounds by neutralising antibody to transforming growth factor β, Lancet, 339, 213-214

Soll, D R, Wessels, D. and Sylwester, A. (1993) The motile behavior of amoebae in the aggregation wave in *Dictyostelium discoideum*, In *Experimental and Theoretical Advances in Biological Pattern Formation*, Othmer, H G, Maini, P K and Murray, J D, (eds.), Plenum Press, London, pp 325-328

Steinbock, O and Müller, S C (1995) Spatial attractors in aggregation patterns of *Dictyostelium discoideum*, *Z. Naturforschung* 50, 275-281

Tang, Y H and Othmer, H G (1994) A G-protein based model of adaptation in *Dictyostelium discoideum*, Math. Biosci., 120, 25-76

Tang, Y H and Othmer, H G (1995) Excitation, oscillations and wave propagation in a G-protein based model of signal transduction in *Dictyostelium discoideum*, Phil. Trans. R. Soc. Lond. B 349, 179-195

Tomchik K J and Devreotes P N (1981) Adenosine 3',5'-Monophosphate waves in *Dictyostelium discoideum*: a demonstration by isotope dilution-fluorography, Science, 212, 443-446

Tyson, J J, Alexander, K A, Manoranjan, V S and Murray, J D (1989) Spiral waves of cyclic AMP in a model of slime mold aggregation, Physica D, 34, 193-207

Tyson, J J and Keener, J P (1988) Singular perturbation theory of traveling waves in excitable media (a review), Physica D, 32, 327-361

Tyson, J J and Murray, J D (1989) Cyclic AMP waves during aggregation of *Dictyostelium* amoebae, Development, 106, 421-426

Van Oss, C, Panfilov, A V, Hogeweg, P, Siegert, F and Weijer, C J (1996) Spatial pattern formation during aggregation of the slime mould *Dictyostelium discoideum*, J. theor. Biol. (to appear)

Vasiev, B N, Hogeweg, P and Panfilov, A V (1994) Simulation of *Dictyostelium discoideum* aggregation via reaction-diffusion model, Phys. Rev. Lett., 73, 3173-3176

Wakefield, L M, Smith, D M, Flanders, K C and Sporn, M B (1988) Latent transforming growth factor β from human platelets, J. Biol. Chem., 263, 7646-7654

Wakefield, L M, Winokur, T S, Hollands, R S, Christopherson, K and Levinson, A D (1990) Recombinant latent transforming growth factor beta 1 has a longer plasma

half-life in rats than an active transforming growth factor beta 1, and a different tissue distribution, J. Clin. Invest., 86, 1976-1984

Whitby, D J and Ferguson, M W J (1991) Immunohistochemical localization of growth factors in fetal wound healing, Dev. Biol., 147,207-215